# Dynamics of Simian Immunodeficiency Virus SIVmac239 Infection in Pigtail Macaques

Nichole R. Klatt, *National Institutes of Health*
Lauren A. Canary, *National Institutes of Health*
Thomas Vanderford, *Emory University*
Carol L. Vinton, *National Institutes of Health*
Jessica C. Engram, *Emory University*
Richard M. Dunham, *Emory University*
Heather E. Cronise, *National Institutes of Health*
Joanna M. Swerczek, *National Institutes of Health*
Bernard A. P. Lafont, *National Institutes of Health*
Louis J. Picker, *Oregon Health & Science University*

*Only first 10 authors above; see publication for full author list.*

**Journal Title:** Journal of Virology

**Volume:** Volume 86, Number 2

**Publisher:** American Society for Microbiology | 2012-01, Pages 1203-1213

**Type of Work:** Article | Final Publisher PDF

**Publisher DOI:** 10.1128/JVI.06033-11

**Permanent URL:** https://pid.emory.edu/ark:/25593/s5sp8

Final published version: http://dx.doi.org/10.1128/JVI.06033-11

## Copyright information:

JVI Journals.ASM.org

# Dynamics of Simian Immunodeficiency Virus SIVmac239 Infection in Pigtail Macaques

**Nichole R. Klatt,[a] Lauren A. Canary,[a] Thomas H. Vanderford,[b] Carol L. Vinton,[a] Jessica C. Engram,[b] Richard M. Dunham,[b] Heather E. Cronise,[c] Joanna M. Swerczek,[c] Bernard A. P. Lafont,[a] Louis J. Picker,[d] Guido Silvestri,[b] and Jason M. Brenchley[a]**

Laboratory of Molecular Microbiology and Program in Barrier Immunity and Repair, NIAID, NIH, Bethesda, Maryland, USA[a]; Yerkes National Primate Research Center, Emory University, Atlanta, Georgia, USA[b]; Comparative Medicine Branch, NIAID, NIH, Poolesville, Maryland, USA[c]; and Department of Molecular Microbiology, VGTI, Oregon Health & Science University, Beaverton, Oregon, USA[d]

**Pigtail macaques (PTM) are an excellent model for HIV research; however, the dynamics of simian immunodeficiency virus (SIV) SIVmac239 infection in PTM have not been fully evaluated. We studied nine PTM prior to infection, during acute and chronic SIVmac239 infections, until progression to AIDS. We found PTM manifest clinical AIDS more rapidly than rhesus macaques (RM), as AIDS-defining events occurred at an average of 42.17 weeks after infection in PTM compared to 69.56 weeks in RM ($P = 0.0018$). However, increased SIV progression was not associated with increased viremia, as both peak and set-point plasma viremias were similar between PTM and RM ($P = 0.7953$ and $P = 0.1006$, respectively). Moreover, this increased disease progression was not associated with rapid $CD4^+$ T cell depletion, as $CD4^+$ T cell decline resembled other SIV/human immunodeficiency virus (HIV) models. Since immune activation is the best predictor of disease progression during HIV infection, we analyzed immune activation by turnover of T cells by BrdU decay and Ki67 expression. We found increased levels of turnover prior to SIV infection of PTM compared to that observed with RM, which may contribute to their increased disease progression rate. These data evaluate the kinetics of SIVmac239-induced disease progression and highlight PTM as a model for HIV infection and the importance of immune activation in SIV disease progression.**

Simian immunodeficiency virus (SIV) and simian-human immunodeficiency chimera virus (SHIV) infections of pigtail macaques (*Macaca nemestrina*; PTM) have become more widely used models for AIDS pathogenesis in recent years; however, the detailed dynamics of SIVmac239 infection in PTM have not been completely characterized. In contrast, the dynamics of SIV infection in rhesus macaques (*Macaca mulatta*; RM) have been comprehensively studied and described (10, 26, 27, 35, 56). Moreover, previous studies have demonstrated that the course of SIV infection in PTM more closely resembles HIV infection in humans than does SIV infection in RM (3). Thus, a more detailed immunological and virological analysis of SIV infection in PTM is essential.

The use of PTM compared to RM for SIV studies is advantageous for a multitude of reasons. These animals are, in general, larger than RM, with PTM averaging 15 kg for adult males and 10 kg for adult females compared to RM averaging 8 kg for adult males and 6 kg for adult females (http://pin.primate.wisc.edu/factsheets/). Increased overall weight allows for larger volumes of peripheral blood sampling and fewer post-surgical procedure complications. Furthermore, the veterinary staff of the NIH Comparative Medicine Branch routinely observes that captive PTM are more adaptable to and less affected by changes in their environment, such as alternating social environments and veterinary staff. Along these lines, PTM also tend to have less incidence of self-injurious behavior. They also display unique facial expressions as part of their behavior and tend to be more social and interactive with people, making them more cooperative during therapeutic treatment administration and facilitating the ease of clinical assessments. Additionally, PTM are less particular with regard to food items, will more readily accept oral therapeutics, and appear to have fewer episodes of inappetence than RM. Thus, the PTM model is an advantageous model for nonhuman primate studies, particularly those involving multiple sampling and/or therapeutic interventions.

While PTM are a desirable model for AIDS research studies, a thorough evaluation of the dynamics of SIV infection in these animals is needed. Indeed, previous studies have demonstrated that SIV and SHIV infections in PTM are unique from lentiviral infection in RM. Specifically, PTM tend to fairly rapidly progress to AIDS after SIV infection, and this progression is often associated with thrombocytopenia (TCP) (2, 39). Indeed, TCP is also a common manifestation of AIDS in untreated human immunodeficiency virus (HIV)-infected individuals and is likely associated with immune activation but can be treated clinically with anti-inflammatory medications (32, 44). Furthermore, prior to infection with SIV, PTM often have damage to their mucosal integrity, increased microbial translocation, increased immune activation, and decreased frequencies of naïve T cells compared to RM, which may contribute to the increased rates of progression to AIDS observed after SIV infection of PTM (30). In addition, low preinfection levels of central memory T cells have been shown to be predictive of AIDS progression in PTM (39). However, similar to RM and humans, a minority of SIV-infected PTM do not progress to AIDS and maintain a long-term nonprogressor (LTNP) phenotype. Recent comprehensive studies of major histocompatibility complex (MHC) class I genetics in PTM have now well character-

**Received** 16 August 2011 **Accepted** 21 October 2011
**Published ahead of print** 16 November 2011
Address correspondence to Jason M. Brenchley, jbrenchl@niaid.nih.gov.
Supplemental material for this article may be found at http://jvi.asm.org/.

doi:10.1128/JVI.06033-11

ized the MHC class I (Mane) alleles that are present in PTM and have demonstrated that the presence of the Mane-A1*084 allele (formerly known as Mane-A*10) is frequently associated with an LTNP phenotype in PTM, similar to Mamu-A1*001, Mamu-B*008, and Mamu-B*017 alleles in RM (5, 17, 33, 48, 52, 58, 59).

Importantly, in contrast to other nonhuman primate models, PTM are susceptible to many lentiviral infections other than SIV and SHIV, including infection with HIV-1, HIV-2, and simian tropic (stHIV-1) (1, 3, 6, 24, 29, 42, 49, 55, 60), which makes this model invaluable for vaccination and pathogenesis studies. Furthermore, recent characterization of APOBEC and TRIM5$\alpha$ genes in PTM has allowed for the development of minimally chimeric stHIV-1 strains, differing from HIV-1 only in *vif* genes, that persistently infect PTM due to the TRIMCyp fusion protein which PTM harbor rather than TRIM5 (11, 21, 60). Furthermore, the TRIMCyp fusion protein that PTM express may contribute to the relative susceptibility of PTM to various SIVs, including SIVagm and chimeric SHIVs (23, 25, 46). Finally, several studies have demonstrated that PTM are an excellent model for comparative research with nonprogressive natural host models of SIV infection (16, 34, 54). Taken together, PTM are clearly a well-suited model for AIDS research. Thus, the goal of this study was to thoroughly define the virological and immunological characteristics of SIVmac239 infection in a cohort of nine PTM in order to provide standard infection characteristics to the rapidly growing field of PTM AIDS research.

## MATERIALS AND METHODS

**Animals and sample collection.** For this study, 9 PTM (*Macaca nemestrina*) were monitored prior to SIV infection, during acute infection, through chronic infection, and to progression to AIDS (6/9 animals) or scheduled euthanasia after lack of AIDS progression (3/9 animals). PTM were infected intravenously (i.v.) with 3,000 50% tissue culture infective doses ($TCID_{50}$) of SIVmac239. Peripheral blood mononuclear cells (PBMCs) were isolated by gradient centrifugation using lymphocyte separation medium (MP Biomedicals). Comparative RM were also infected with 3,000 $TCID_{50}$ of SIVmac239 i.v. but from different SIVmac239 stocks. Animals were housed and cared in accordance with American Association for Accreditation of Laboratory Animal Care (AAALAC) standards in AAALAC-accredited facilities, and all animal procedures were performed according to protocols approved by the Institutional Animal Care and Use Committees of the National Institute of Allergy and Infectious Diseases, National Institutes of Health, Yerkes National Primate Research Center, Emory University, and the Oregon National Primate Research Center, OHSU.

**Viral loads.** Viral RNA levels in plasma were determined by real-time reverse transcription-PCR (ABI Prism 7700 sequence detection system; Applied Biosystems) using reverse-transcribed viral RNA in plasma samples from SIVmac239-inoculated rhesus macaques as previously described (31).

**Flow cytometry.** Multicolor flow cytometric analysis was performed on samples as previously described (30), using cross-reactive anti-human antibodies CD3 (clone SP34-2; BD Pharmingen), CD8 (RPA-T8; BD Pharmingen), CD4 (OKT4; eBioscience), Ki67 (B26; BD Pharmingen), BrdU (3D4; BD Pharmingen), CCR5 phycoerythrin (PE) (clone 3A9; BD Pharmingen), CD28 ECD (phycoerythrin Texas Red conjugate energy-coupled dye) (clone 28.2; Beckman Coulter), CD95 PE-Cy5 (clone DX2; BD Pharmingen), and Aqua Live/Dead amine dye (Invitrogen). Flow cytometric acquisition was performed on a BD LSRFortessa cell analyzer driven by FACSDiVa software (v6.0; BD). Analysis of the acquired data was performed using FlowJo software (v9.0.2; TreeStar). We used a minimum threshold of 200 collected events in the final populations measured for all analyses.

**BrdU labeling and staining.** A total of 30 mg of BrdU per kg of body weight diluted in Hank's medium (Cellgro) was administered i.v. to each PTM for 5 consecutive days prior to SIV infection, during acute SIV infection, and during chronic SIV infection, at least 90 days from the prior administration. PBMCs were frozen during washout, and all samples were thawed and stained for BrdU labeling at the same time for consistency. PBMCs were first stained with predetermined optimal concentrations of surface antibodies (surface antibodies conjugated to Pacific Blue must be incubated after the BrdU stain) for 20 min, and then 1 ml of 1$\times$ fluorescence-activated cell sorter (FACS) lysing solution (BD Pharmingen) was added directly to the surface stain, incubated for 6 min at room temperature, and then washed with phosphate-buffered saline. Next, cells were permeabilized with Cytofix/Cytoperm (BD Pharmingen) for 20 min, followed by two washes with Cytofix/Cytoperm wash buffer (BD Pharmingen). Intracellular antibodies Ki67 and BrdU were subsequently incubated for 30 min at 37°C with 30 $\mu$g DNase (Sigma) and then washed with BD Cytofix/Cytoperm wash buffer. Finally, Pacific Blue-conjugated antibodies were added last and incubated for 20 min, then washed with BD Cytofix/Cytoperm wash buffer, and fixed with 1% paraformaldehyde (Electron Microscopy Systems). Samples were then analyzed by flow cytometry as described below.

**Intracellular cytokine assay.** Stimulation of antigen-specific T cells was performed on frozen lymphocytes as described previously (51). Freshly thawed lymphocytes were resuspended at $10^6$ cells/ml in RPMI medium supplemented with antibiotics and glutamine. Anti-CD28 conjugated to Alexa Fluor 594 PE and unconjugated antibodies to CD49d were used for costimulation. A negative control (cells treated only with costimulatory anti-CD28 and anti-CD49d) was included for every experiment. Peptides used to stimulate SIV-specific T cells were 15 amino acids in length, overlapping by 11 amino acids, and encompassed SIVmac230 Gag (New England Peptide). The concentration of each individual peptide was 2 $\mu$g/ml for stimulations. All stimulations were preformed in the presence of brefeldin A (BFA) (1 $\mu$g/ml; Sigma) for 16 h at 37°C. All cells were surface stained with the dead cell exclusion dye Aqua Blue (Invitrogen), followed by surface staining with anti-CD3 Alx700 (BD), anti-CD4 Cy5.5 PE (eBiosciences), anti-CD8 Pacific Blue (BD), and anti-CD95 Cy5 PE (BD). Cells were then fixed and permeabilized, followed by intracellular staining with anti-gamma interferon (anti-IFN-$\gamma$) Cy7PE (BD), anti-interleukin-2 (anti-IL-2) allophycocyanin (APC) (BD), and tumor necrosis factor (TNF) fluorescein isothiocyanate (FITC) (BD). SIV-specific $CD8^+$ and $CD4^+$ T cell responses are reported as the frequency of memory $CD8^+$ or $CD4^+$ T cells, gated by characteristic light-scattering properties, the frequency of Aqua Blue, $CD3^+$, $CD8^+$, $CD4^+$, or $CD95^+$ cells, and the production of any combination of effector cytokines (based upon Boolean gating). All data are reported after background subtraction.

SIV stimulation of PDCs was performed on frozen lymphocytes as described previously (38). Freshly thawed lymphocytes were resuspended at $10^6$ cells/ml in RPMI medium supplemented with antibiotics and glutamine. A total of 500 ng/ml aldrithiol-2-inactivated SIVmac239 was used to stimulate plasmacytoid dendritic cells (PDCs). A negative control was included for every experiment. All stimulations were performed in the presence of BFA for 16 h at 37°C. All cells were surface stained with the dead cell exclusion dye Aqua Blue (Invitrogen), followed by surface staining with anti-CD3 FITC, CD20 FITC, CD56 FITC, CD16 FITC, HLA-DR H7APC, CD123 Pacific Blue, and CD11c Cy5 PE. Cells were then fixed and permeabilized, followed by intracellular staining with anti-TNF APC. Frequencies of responding PDCs are reported after gating by characteristic light-scattering properties, Aqua Blue, lineage-negative, HLA-$DR^+$, $CD123^+$, or $CD11c^+$ cells, and production of TNF. All data are reported after background subtraction.

**Analysis of KP9 epitope evolution.** Viral RNA from plasma samples collected during the acute and chronic phases (day 14 and days 162 to 205 post-SIV infection, respectively) was extracted using a QIAamp viral RNA minikit (Qiagen, Valencia, CA) by following the manufacturer's instructions. The SuperScript III first strand synthesis system (Invitrogen, Carls-

**TABLE 1** Pathology of SIV-infected pigtail macaques at death/euthanasia

| Animal | Age at SIVmac239 infection (yr) | Mane-A1*084$^+$ | Days post-SIV infection at death | AIDS symptoms at death[a] |
|---|---|---|---|---|
| PT98P030 | 11 | Yes | 733 | Scheduled euthanasia/LTNP |
| PT99P030 | 10 | Yes | 729 | Scheduled euthanasia/LTNP |
| PTA1P012 | 8 | Yes | 727 | Scheduled euthanasia/LTNP |
| PTA0P012 | 9 | No | 343 | Thrombocytopenia, anemia, low albumin, diarrhea, lung adhesions, liver adhesion, lymphadenopathy (particularly in mesenteries), ventricular thrombus |
| PTA0P007 | 9 | Yes | 329 | Thrombocytopenia, lymphadenopathy, *Moraxella* infection |
| PT99P029 | 10 | No | 273 | Thrombocytopenia, acute respiratory distress, lymph nodes near trachea, *Pneumocystis* pneumonia |
| PT98P005 | 11 | No | 191 | Thrombocytopenia, cytomegalovirus vasculitis, swelling of appendages |
| PT99P052 | 10 | Yes | 322 | Severe diarrhea, thrombocytopenia, ventricular thrombus, lung adhesions, lymphadenopathy |
| PTA0P039 | 9 | No | 315 | Severe diarrhea, nodules on colon, liver adhesions, enteritis |

[a] Thrombocytopenia is defined as <100 platelets/mm$^3$ blood.

bad, CA) was used to generate viral cDNA. Briefly, viral RNA mixed with 50 ng of random hexamers and 1 mM deoxynucleoside triphosphate (dNTP) was incubated at 70°C for 5 min. After 5 min on ice, the cDNA was synthesized in a reaction consisting of 20 mM Tris-HCl (pH 8.4), 50 mM KCl, 5 mM $MgCl_2$, 10 mM dithiothreitol (DTT), 500 $\mu$M each dNTP, 40 U RNaseOUT, and 200 U SuperScript III reverse transcriptase (RT). The reaction mixture was incubated at 50°C for 50 min. The RT was inactivated for 5 min at 85°C, and cDNA was treated with RNase H for 20 min at 37°C.

The SIV Gag region encoding the KP9 epitope was amplified by PCR using cDNA as described previously (18). Briefly, cDNA generated from plasma viral RNA was amplified with SIV Gag no. 4 (5′ CAGGCAGAAG AGAAAGTGAA 3′) and SIV Gag no. 5 (5′ GTTCCTGCAATRTCKG ATCC 3′) primers and Phusion high-fidelity DNA polymerase (Finnzymes) according to the manufacturer's instructions. The PCR conditions were 98°C for 30 s, followed by 35 cycles at 98°C for 10 s, 56°C for 20 s, and 72°C for 30 s, and a final incubation at 72°C for 7 min. The 452-bp fragment was gel purified on a 1.2% agarose gel using a QIAquick gel extraction kit (Qiagen), and the purified product was directly sequenced using a 3130XL genetic analyzer (Applied Biosystems).

**Statistical analysis.** We performed a Mann-Whitney U test for all *t* test *P* values, except for the results in Fig. 1 where we used the Gehan-Beslow-Wilcoxon test. Horizontal bars in figures reflect medians. All statistics were performed using Prism 5.0 software.

## RESULTS

**SIVmac239 infection results in rapid progression to AIDS in PTM compared to RM but not due to increased viral loads.** In order to determine the length of time between infection with SIVmac239 and progression to AIDS in PTM, we infected 9 PTM with 3,000 $TCID_{50}$ of SIVmac239 i.v. Animals were allowed to progress through infection without intervention, until clinical AIDS occurred in 6 of 9 of the animals (Table 1). On average, the six PTM that displayed progressive SIV infection progressed to AIDS-defining illnesses (Table 1) at 42.17 weeks after SIV infection (Fig. 1). In contrast, in 14 RM (without protective MHC alleles) also infected with SIVmac239 i.v., AIDS progression occurred at an average of 69.56 weeks after SIV infection, significantly later than in PTM ($P = 0.0018$; Fig. 1). Of note, the 3 PTM that did not progress to AIDS all expressed the protective Mane-A1*084 allele, as did 2 of the animals that progressed to AIDS (Table 1).

In order to define the kinetics and magnitude of SIVmac239 replication in our cohort of PTM and to determine whether increased AIDS progression rates were associated with increased viremia in PTM, we closely monitored plasma viral loads during acute and chronic stages of infection and AIDS (Fig. 2A and B). Three of six PTM (98P030, 99P030, and A1P012), all of which had Mane-A1*084 alleles (Table 1), had decreasing viral loads as infection persisted, despite high peak viral loads (Fig. 2B), and had not progressed to AIDS after more than 700 days postinoculation. Therefore, these three Mane-A1*084$^+$ PTM were classified as LTNP and had scheduled euthanasia at days 733, 729, and 727, respectively.

Peak viremia in PTM occurred near day 14 postinfection (Fig. 2A and B), with an average of 6.28 SIV copies/ml plasma ($\log_{10}$) in PTM, similar to 6.29 SIV copies/ml plasma ($\log_{10}$) in RM ($P = 0.7953$; Fig. 2C). However, while day 14 viral loads were peak for PTM, and similar to day 14 levels for RM, RM hit peak earlier, at day 10 post-SIVmac239 infection, and was at a higher peak than PTM, with an average viral load of 7.58 copies/ml plasma ($\log_{10}$) in RM at day 10 compared to 5.93 SIV copies/ml plasma in PTM ($P = 0.0016$; Fig. 2B). However, of note, a higher peak viral load could have occurred in PTM at a time point that was not measured. Set-point viremia in PTM, however, tended to be moder-

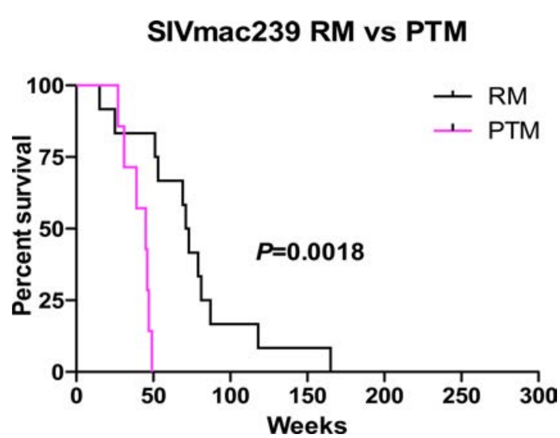


**FIG 1** Pigtail macaques progress to AIDS more rapidly than rhesus macaques. Survival, as measured by weeks until AIDS-defining illnesses and death, in 6 PTM (purple) compared to 14 RM (black) after SIVmac239 infection. The *P* value was determined using the Gehan-Breslow-Wilcoxon test.

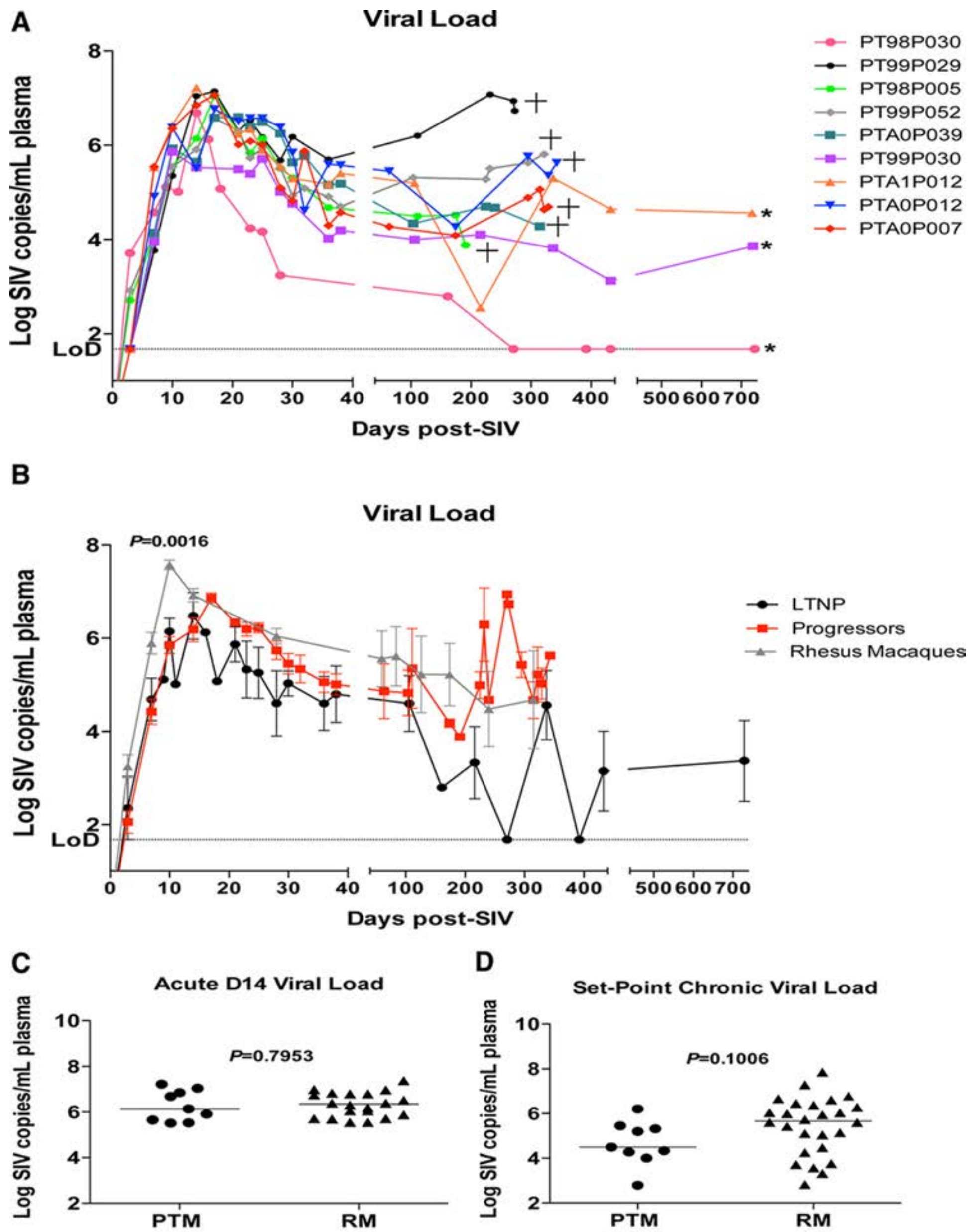


**FIG 2** Dynamics of SIV plasma viremia in pigtail macaques. (A and B) Plasma viral loads were measured by RT-PCR throughout infection in PTM (limit of detection [LoD] was 1.68 $\log_{10}$ copies SIV/ml plasma). (A) Individual plasma viral loads throughout infection. Crosses represent death due to AIDS-defining illness, and stars represent scheduled euthanasia in LTNPs. (B) Average viral loads throughout infection for PTM progressors (red) compared to those for PTM LTNPs (black) and RM (gray) through chronic infection (not AIDS). (C) Levels of viremia at day 14 postinfection in PTM (circles) compared to those in RM (triangles). (D) Set-point levels of viremia during chronic (100+ days postinfection) SIVmac239 infection in PTM (circles) compared to those in RM (triangles). (C and D) The horizontal line represents the median, and *P* values were determined using the Mann-Whitney nonparametric *t* test.

ately lower than observed in RM (Fig. 2B and D), with an average of 4.67 SIV copies/ml plasma ($\log_{10}$) in PTM compared to 5.51 SIV copies/ml plasma (log10) in RM at set point ($P = 0.1006$; Fig. 2D). Thus, increased SIVmac239 replication does not account for increased disease progression rates in PTM. Furthermore, similar kinetics and magnitudes of plasma viremia were observed in additional PTM infected with SIVmac239 in independent studies (see Fig. S1 in the supplemental material).

**$CD4^+$ T cells are depleted from the periphery of PTM after SIV infection.** To determine the kinetics of peripheral blood $CD4^+$ T cell depletion in PTM and RM after SIVmac239 infection, we measured the frequency of $CD4^+$ T cells by flow cytometry frequently throughout the infection and at time of death (AIDS or scheduled for euthanasia). Prior to SIV infection, PTM had an average of 45.54% $CD4^+$ T cells but at time of death had an average of 28.81% $CD4^+$ T cells (Fig. 3A). Furthermore, the loss of $CD4^+$ T cells at death was lower in animals that progressed to AIDS (average, 25.9%) than in the three LTNPs (average, 34.63%) that were scheduled for euthanasia ($P = 0.2619$; Fig. 3C). The loss of $CD4^+$ T cells was particularly apparent when numbers of cells

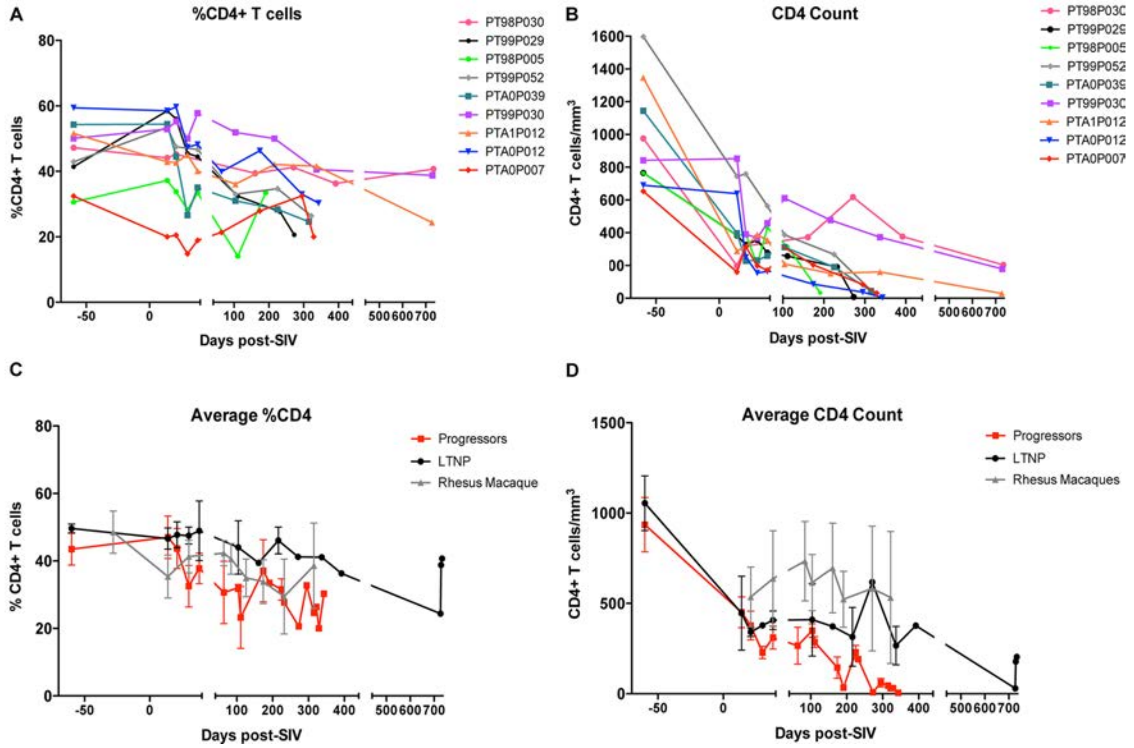


**FIG 3** CD4$^+$ T cells are progressively depleted during SIV infection of pigtail macaques. The fraction of CD4$^+$ T cells in peripheral blood was assessed by flow cytometry, gated on live, singlet, CD3$^+$ lymphocytes. (A) Fraction of CD4$^+$ T cells throughout infection in individual animals. (B) The absolute number of CD4$^+$ T cells/mm$^3$ of blood was assessed by flow cytometry and complete blood cell counts (CBC) of lymphocytes throughout infection. (C) Average fraction of CD4$^+$ T cells in progressors (red), LTNPs (black) throughout infection, and RM (gray) through chronic infection (not AIDS). (D) Average absolute number of CD4$^+$ T cells/mm$^3$ in progressors (red), LTNPs (black), and RM (gray).

per mm$^3$ of blood were calculated and compared to the depletion of CD4$^+$ T cells from chronically SIV-infected RM (Fig. 3D). Indeed, prior to SIV infection, PTM maintained an average of 975.39 CD4$^+$ T cells/mm$^3$ in peripheral blood (Fig. 3B). However, at time of death, the loss of CD4$^+$ T cells was dramatic, with an average of only 62.53 CD4$^+$ T cells/mm$^3$ in peripheral blood. Again, this loss was more dramatic in animals which progressed to AIDS, with an average of 25.21 CD4$^+$ T cells at time of death compared to 137.16 CD4$^+$ T cells in LTNPs ($P = 0.2619$; Fig. 3D), though the ultimate loss of CD4$^+$ T cells despite decreased viremia in the three LTNP PTM was surprising. However, overall, the loss of CD4$^+$ T cells throughout infection is similar to the dynamics of CD4$^+$ T cell loss during both SIVmac239 infection of RM (Fig. 3C and D) (15, 50) and HIV-1 infection of humans (8, 13), albeit the complete loss of CD4$^+$ T cells in PTM occurs at a more rapid pace despite similar/lower viral loads, consistent with their increased disease progression rates.

**Memory CD4$^+$ T cells and CCR5$^+$ memory CD4$^+$ T cells are rapidly lost in blood after SIV infection of PTM.** Because SIVmac239 preferentially infects CD4$^+$ memory T cells, specifically those which express the coreceptor CCR5 (40), we measured the frequencies of memory/effector CD4$^+$ T cells by flow cytometry (CD4$^+$ CD28$^+$ CD95$^+$ and CD4$^+$ CD28$^-$), as well as the frequency of CCR5+ cells within the memory/effector CD4$^+$ T cell subsets. After SIV infection, similar to what has been described for RM (40, 47) and humans (13), the fraction of memory/effector CD4$^+$ T cell subsets declined rapidly; however, a slight increase in the fraction of memory/effector CD4$^+$ T cells was observed at time of death (Fig. 4A). This increase in frequency was not due to increased numbers of memory/effector CD4$^+$ T cells, as the absolute number of these cells rapidly and persistently declined in all animals (Fig. 4B). Thus, the increased frequency of CD4$^+$ memory/effector T cells at time of death is likely due to a loss of naïve CD4$^+$ T cells with a presumable inability to maintain the memory CD4$^+$ T cell pool.

Similar to what has been described during acute HIV infection in humans (61), CCR5$^+$ memory/effector CD4$^+$ T cells were massively and rapidly depleted after SIV infection of PTM (Fig. 4C and D). However, during chronic infection, both the frequency and number of CCR5$^+$ CD4$^+$ T cells increased compared to those during acute infection but declined again when the PTM progressed to AIDS (Fig. 4C and D). Of interest, however, two of the three LTNP animals (99P030 and A1P012) increased the frequency and number of CD4$^+$ CCR5$^+$ T cells more rapidly than the progressing PTM after the initial loss, and the third LTNP (98P030) did not lose any CD4$^+$ CCR5$^+$ memory/effector T cells during acute infection.

**Rapid SIV progression in PTM is associated with increased levels of T cell turnover prior to infection.** Immune activation is the strongest predictor of disease progression rates during HIV infection of humans (19, 22) and SIV infection of RM (57). Thus, we evaluated immune activation prior to and throughout the course of SIV infection in PTM. As previously described (30), we observed increased immune activation as measured by Ki67 expression by T cells prior to SIV infection in PTM compared to levels observed in uninfected RM (Fig. 5A). On average, prior to

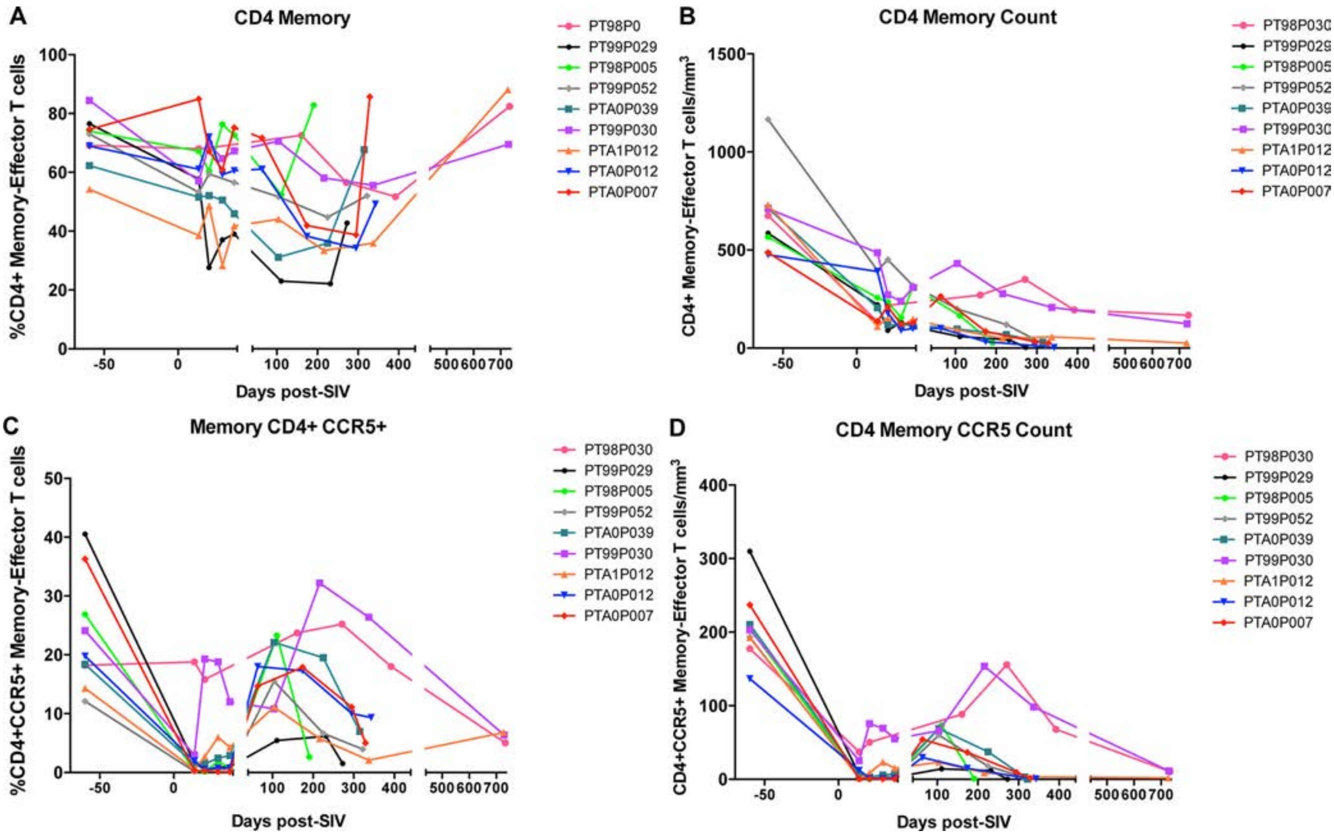


**FIG 4** SIVmac239 infection in pigtail macaques results in depletion of memory/effector CD4$^+$ T cells and CCR5$^+$ CD4$^+$ T cells. Fractions of memory/effector CD4$^+$ T cells (CD28$^+$ CD95$^+$ and CD28$^-$ CD4$^+$ T cells) and CCR5$^+$ memory/effector CD4$^+$ T cells in peripheral blood were assessed by flow cytometry. (A) Fraction of memory/effector CD4$^+$ T cells throughout infection. (B) The absolute number of memory/effector CD4$^+$ T cells/mm$^3$ was calculated using lymphocyte CBC. (C) Fraction of CCR5$^+$ memory/effector CD4$^+$ T cells throughout infection. (D) The absolute number of CCR5$^+$ memory/effector CD4$^+$ T cells/mm$^3$ was calculated using lymphocyte CBC.

SIV infection, 17.63% of CD4$^+$ memory/effector T cells expressed Ki67 (Fig. 5A, left) and 13.07% of CD8$^+$ memory/effector T cells expressed Ki67 (Fig. 5A, right). In comparison, in RM, the average Ki67 expression by CD4$^+$ memory/effector T cells prior to SIV infection is 1.2% ($P = 0.0033$) and by CD8$^+$ memory/effector T cells is 1.2% ($P = 0.0010$). During acute SIV infection, the fraction of Ki67$^+$ CD4$^+$ memory/effector T cells rapidly increased to levels much higher than observed in RM (day 14; $P = 0.0010$) (Fig. 5A, left and center). The fraction of Ki67$^+$ CD8$^+$ memory/effector T cells also rapidly increased in PTM, similar to that in RM (day 14; $P = 0.0599$) (Fig. 5A, right). Furthermore, consistent with HIV and SIV preferentially infecting proliferating memory CD4$^+$ T cells (7, 12, 41), the absolute number of Ki67$^+$ CD4$^+$ memory/effector T cells rapidly declined after SIV infection (Fig. 5A, center). Following rapid depletion of proliferating CD4$^+$ memory/effector T cells, the number of these cells then increased during the chronic phase of infection, consistent with increased immune activation (Fig. 5A). However, as the PTM ultimately progressed throughout chronic infection and to AIDS, the number of Ki67$^+$ CD4$^+$ memory/effector T cells progressively declined (Fig. 5A, center), likely due to infection by SIV, as well as constant strain placed on the T cell pool.

In order to assess T cell turnover during SIVmac239 infection, we administered bromodeoxyuridine (BrdU), a thymidine analogue, to PTM prior to infection, during acute infection (days 14 to 18 post-SIV infection), in order to label cells during the peak activation and viremia time points, and during chronic infection (150 to 190 days post-SIV infection). We evaluated T cell turnover by measuring the fraction of memory/effector T cells retaining BrdU over time (see Fig. S2 in the supplemental material). The decay kinetics of BrdU$^+$ T cells in uninfected PTM revealed high levels of turnover in both CD4$^+$ (Fig. 5B, left) and CD8$^+$ (Fig. 5C, left) memory/effector T cell populations. Previous studies of BrdU decay kinetics in RM have demonstrated that SIV infection results in a profound increase in turnover of memory T cells during both acute and chronic phases of SIVmac239 infection compared to turnover in uninfected RM (50). In contrast, in PTM, we found that 10 days following BrdU administration in uninfected PTM, on average only 36.33% of memory/effector CD4$^+$ T cells maintained BrdU (thus, 63.67% of these cells had proliferated and/or died) (Fig. 5B, left) and 54.45% of CD8$^+$ memory/effector T cells maintained BrdU (thus, 45.55% had proliferated) (Fig. 5C, left). Surprisingly, during acute SIV infection, turnover of memory/effector CD4$^+$ T cells was somewhat decreased compared to that during pre-SIV infection, with an average of 52.60% turnover 10 days after BrdU administration (Fig. 5B, center). Furthermore, acute-phase turnover of CD8$^+$ memory/effector T cells was similar to preinfection levels, with 50.61% of cells maintaining BrdU after 10 days (Fig. 5C, center). This is in contrast to SIVmac239 infection of RM, where it has been shown that the highest levels of

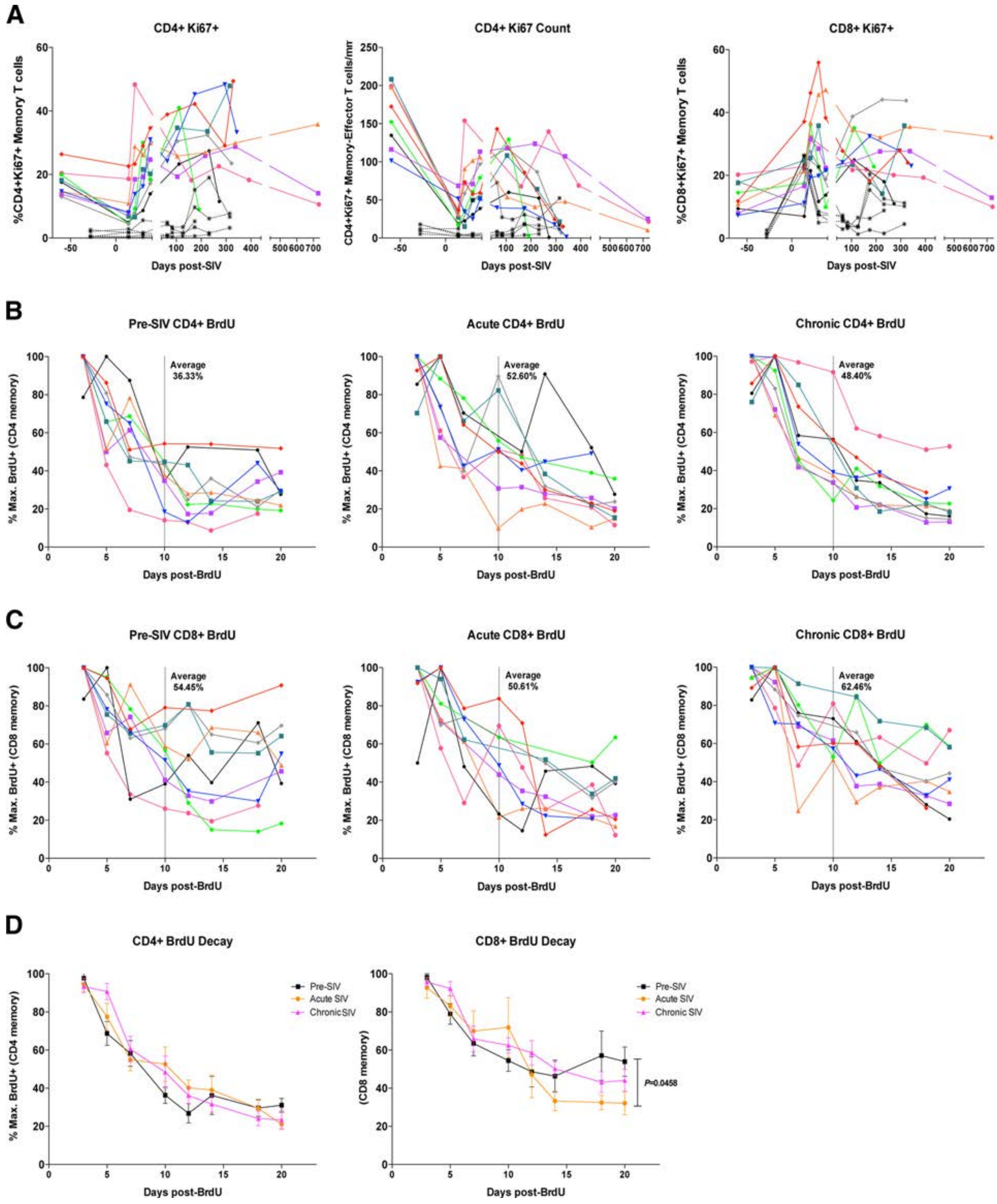


**FIG 5** Pigtail macaques have high levels of proliferation and turnover prior to SIVmac239 infection. (A) Proliferation of T cells in peripheral blood was assessed by the expression of Ki67, measured by flow cytometry on CD4$^+$ memory/effector T cells (A, left) and CD8$^+$ memory/effector T cells (A, right). (A, center) The absolute number of Ki67$^+$ memory/effector CD4$^+$ T cells/mm$^3$ was calculated by lymphocyte CBC. (B to D) Turnover of T cells was measured by BrdU decay kinetics. BrdU was administered at 30 mg/kg for 5 consecutive days in each animal prior to SIV infection, during acute SIV infection (1st day of BrdU administration, day 14 post-SIV infection), and during chronic SIV infection (150 to 190 days post-SIV infection). The first sampling occurred 3 days after the last day of BrdU infusion. Decay is measured by the fraction of maximally labeled BrdU$^+$ cells. BrdU expression was measured by flow cytometry on CD4$^+$ memory/effector T cells (B) or CD8$^+$ memory/effector T cells (C). (B and C) The dotted vertical line represents 10 days after BrdU administration, with the average fraction of maximum BrdU$^+$ cells notated. (D) Labeling of average turnover during pre-SIV (black), acute SIV (orange), and chronic SIV (purple) infections in CD4$^+$ memory/effector T cells (left) and CD8$^+$ memory/effector T cells (right).

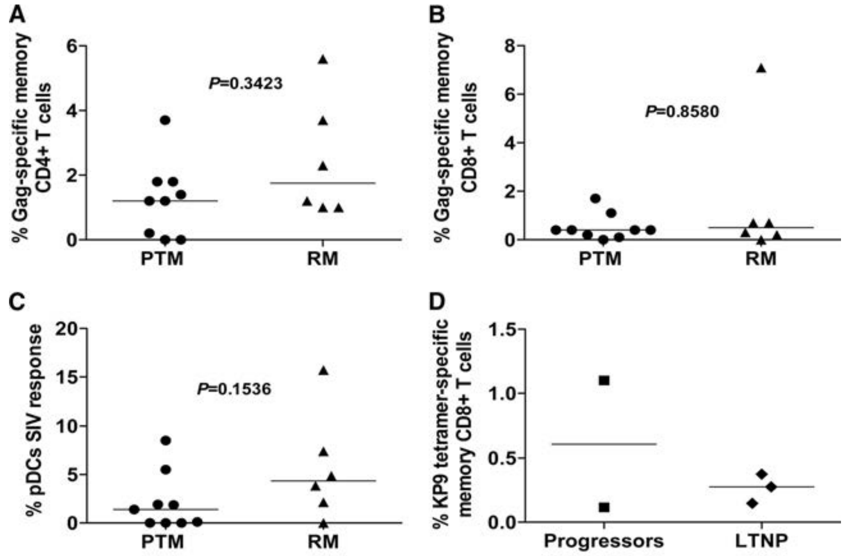


E

| Animal | Status | A1*084 | KP9 D14 | KP9 Chronic |
|---|---|---|---|---|
| PT99P030 | LTNP | POSITIVE | KKFGAEVVP | KXFGAEVVX* |
| PTA1P012 | LTNP | POSITIVE | KKFGAEVVP | KRFGAEVVP |
| PTA0P007 | Progressor | POSITIVE | KKFGAEVVP | KKFGAEVVS |
| PT99P052 | Progressor | POSITIVE | KKFGAEVVP | KRFGAEVVP |
| PT98P005 | Progressor | Negative | KKFGAEVVP | KKFGAEVVP |
| PTA0P012 | Progressor | Negative | KKFGAEVVP | KKFGAEVVP |

*K(K>R)FGAEVV(S>P)

**FIG 6** Immune responses to SIV and escape from SIV Gag in pigtail macaques. (A and B) The frequencies of memory/effector $CD4^+$ (A) and $CD8^+$ (B) T cells that produced cytokines in response to SIV Gag peptide stimulation were measured by flow cytometry. (C) The frequency of lineage-negative, HLA-$DR^+$ $CD11c^-$ $CD123^+$ pDCs that produced TNF-$\alpha$ after stimulation with chemically inactivated SIV (AT2) was measured by flow cytometry. (D) The frequency of memory/effector $CD8^+$ T cells from ManeA1*084+ PTM which bound the SIV Gag KP9 tetramer was measured by flow cytometry. (E) SIVmac239 Gag was sequenced, and the KP9 epitope was analyzed for escape from the wild type (KKFGAEVVP). Red letters reflect mutations in the KP9 sequence. (A to C) PTM, circles; RM, triangles. The horizontal line represents the median, and *P* values were determined using the Mann-Whitney nonparametric *t* test. (D) PTM progressors, squares; PTM LTNPs, diamonds. The horizontal line represents the median.

turnover occur during acute infection, with approximately 20% of memory T cells maintaining BrdU 10 days after washout, compared to approximately 60% of memory T cells maintaining BrdU 10 days after washout prior to SIV infection (50). Furthermore, in chronic SIV infection of PTM, we again found decreased levels of turnover compared to those during preinfection, with an average of 48.40% of $CD4^+$ memory/effector T cells (Fig. 5B, right) and 62.46% of $CD8^+$ memory/effector T cells (Fig. 5C, right) maintaining BrdU after 10 days. This is again in contrast to SIV infection of RM, in which approximately 30% of memory T cells maintain BrdU after 10 days, demonstrating increased turnover compared to that in uninfected RM (50). The lack of differential turnover at different phases of infection in PTM is highlighted by comparisons of the average turnover levels of all animals at each phase (Fig. 5D). In both $CD4^+$ and $CD8^+$ memory/effector T cells, the rates of BrdU decay are similar regardless of infection phase or status, with a trend toward pre-SIV infection decay being more rapid (Fig. 5D). Of note, however, prior to SIV infection in $CD8^+$ memory/effector T cells (Fig. 5D, right), after 12 days post-BrdU administration, decay wanes, whereas during acute and chronic infections, decay rates continue through the end of measurements (day 20 post-BrdU administration) and are significantly different between pre-SIV and acute SIV infection time points at day 20 ($P = 0.0458$). Taken together, PTM clearly have high levels of turnover and proliferation of T cells prior to SIV infection compared to previous reports for RM (50), which may contribute to the increased disease progression rates after SIVmac239 infection in these animals.

**Rapid progression in PTM is not due to decreased SIV-specific immune responses compared to those in RM.** In order to determine whether rapid progression in PTM was due to low frequencies of SIV-specific immune responses, we stimulated PTM and RM PBMCs with SIV Gag peptides and measured the frequency of SIV-specific T cells. We found measurable memory/effector $CD4^+$ T cell responses to Gag peptides in 7 of 9 PTM and in 6 chronically SIVmac239-infected RM (Fig. 6A). However, the frequency of SIV-specific memory/$CD4^+$ T cells was not significantly different in PTM than in RM ($P = 0.3423$) (Fig. 6A). Similarly, 8 of 9 PTM and 5 of 6 RM had measurable SIV-specific memory/effector $CD8^+$ T cells, but again, no difference was observed between species ($P = 0.8580$) (Fig. 6B). We also assessed innate immune responses by measuring the frequency of lineage-negative, HLA-$DR^+$ $CD11c^-$ $CD123^+$ plasmacytoid dendritic cells (pDCs) that produced TNF-$\alpha$ in response to chemically inactivated SIV (AT2) stimulation. We found measurable frequencies of pDCs responding to AT2-inactivated SIV in 6 of 9 PTM and 5 of 6 RM, and while there was a trend for an increased frequency of pDCs that responded to SIV in RM, the difference between species was not significantly different ($P = 0.1536$) (Fig. 6C).

We further assessed SIV-specific immune responses in PTM by measuring the frequencies of memory/effector $CD8^+$ T cells which bound ManeA1*084 tetramers loaded with the KP9 epitope, which is an immunodominant SIV Gag epitope presented by the ManeA1*$084^+$ allele (59). In all 5 ManeA1*$084^+$ PTM, we observed measurable KP9-specific $CD8^+$ T cells; however, we observed no significant differences between ManeA1*$084^+$ PTM that progressed and LTNP animals (Fig. 6D). Hence, increased frequencies of KP9-specific $CD8^+$ T cells are unlikely the mechanism underlying the LTNP phenotype we observed. Moreover, previous studies have demonstrated that escape from the KP9 epitope by the virus infecting ManeA1*$084^+$ PTM has been shown to result in loss of SIV fitness *in vivo* (18, 36). Thus, to assess whether escape from the KP9 epitope by SIVmac239 occurred in the ManeA1*$084^+$ PTM and whether differential viral escape may explain differences between progressors and LTNPs, we sequenced SIV from the plasma of several SIV-infected PTM and analyzed immune escape within KP9 during acute infection (day 14 post-SIV infection) and chronic infection (days 148 to 191 post-SIV infection) (Fig. 6E). As expected, the ManeA1*$084^-$ PTM analyzed did not have immune escape in KP9; however, all 4 ManeA1*084 PTM analyzed exhibited escape within KP9 during chronic but not acute infection (Fig. 6E). Thus, selective escape from the KP9 Gag epitope in LTNPs does not explain the lack of progression in these animals, nor does acute escape from KP9 explain rapid progression in our cohort of PTM.

## DISCUSSION

*Macaca nemestrina* (PTM) has become increasingly used as an invaluable model for AIDS virus pathogenesis studies; however, the characteristics of SIV infection in this Asian primate have not been comprehensively defined. Here, we evaluated the dynamics of SIVmac239 infection in PTM prior to infection, during acute infection, and throughout chronic infection until animals succumbed to simian AIDS. We found that in comparison to RM, PTM progress more rapidly to AIDS-defining illnesses after SIVmac239 infection, but this accelerated rate of disease progression was not attributed to increased peak or set-point plasma viral loads. This is of interest, as previous studies have demonstrated that SHIV, HIV-1, and HIV-2 replicate at extremely high levels in pigtail macaques (3, 6, 24, 42, 49), and SIVagm replicates at variable levels (20). However, somewhat lower SIVmac239 replication rates followed by progression to AIDS are consistent with the immunodeficiency that is observed in PTM after infection with SIVsun or SIVhoest, where animals progress to AIDS despite low levels of viremia (4). Taken together, however, these data indicate that levels of peak and set-point viremia by themselves do not dictate the rate of progression to AIDS in PTM and that a variety of virological and immunological factors likely contribute to levels of acute and set-point viremia.

Similar to that observed in humans and RM, $CD4^+$ T cell depletion in peripheral blood occurs in PTM after SIV infection, albeit at a more rapid pace, consistent with the observed rapid progression to AIDS. Also similar to SIV infection in RM and HIV infection in humans, massive depletion specifically occurred in memory/effector $CD4^+$ T cell and $CCR5^+$ memory/effector $CD4^+$ T cell subsets, an observation which is consistent with the CCR5 tropism of SIVmac239 (13, 14, 40, 45). In contrast to HIV-uninfected humans and SIV-uninfected RM, we found that SIV-uninfected PTM had high levels of proliferation and turnover in the memory/effector T cell compartments.

Three of the nine PTM studied displayed an LTNP-like phenotype, all of which expressed Mane-A1*084. These animals maintained lower viral loads and higher levels of $CD4^+$ T cells and at time of scheduled euthanasia (non-AIDS related) had survived nearly twice as long as the other 6 progressing PTM ($P = 0.0238$). However, at time of euthanasia, $CD4^+$ T cells in LTNPs started to be depleted, and thus, these animals may have eventually progressed to AIDS. This phenomenon has also been observed in HIV-infected elite controllers, where these individuals lose $CD4^+$ T cells and have higher immune activation levels than HIV-uninfected individuals, despite low levels of viremia (22). Thus, SIVmac239 infection in LTNP-like Mane-A1*$084^+$ PTM may be valuable as a model for studying HIV-infected elite controllers.

It is of interest that while PTM have higher preinfection levels of immune activation than RM, the levels of T cell proliferation after SIV infection are similar to those observed in RM, and levels of T cell turnover actually tend to be lower than those observed in RM (50). A previous report by Mason et al. (39) suggested that preinfection levels of central memory T cells correlated with increased disease progression rates in PTM. However, we expand on that finding here, demonstrating that the overall rapid turnover and proliferation in T cell subsets in PTM regardless of infection status likely contribute to disease progression. Furthermore, we have previously reported (30) that prior to SIV infection in PTM, there is increased damage to the gastrointestinal tract, microbial translocation, and immune activation compared to that observed prior to infection in RM, all of which may contribute to the increased mortality observed here. However, why this increased activation and turnover exist and precisely how this may contribute to rapid SIV progression in PTM should be more thoroughly investigated, including the study of mucosal immunity during SIV infection in PTM.

Overall, the dynamics of SIVmac239 infection in PTM are similar to the dynamics of HIV infection in humans and SIV infection in RM. However, this model provides many benefits as an alternate to using RM. First, the increased disease progression rate can be an asset when testing vaccination strategies and/or therapeutic interventions, as it will shorten the length of follow-up time during studies, thus expediting results and fraying expensive cage charges. Second, as discussed above, PTM tend to be larger and more receptive and cooperative to therapeutic strategies, thus making them ideal in large-scale, intensive sampling studies. Third, these animals are susceptible to a greater breadth of chimeric SIV and even HIV strains. Finally, the increased immune activation in PTM prior to SIV infection may better capitulate overall HIV infection, as the majority of HIV infections occur in developing countries, such as Africa, where individuals tend to have higher baseline levels of immune activation than individuals in developed countries (9, 28, 37, 43, 53). Thus, taken together, PTM are an excellent model for HIV/AIDS pathogenesis, vaccine, and therapeutic studies, and the evaluation of SIVmac239 infection in PTM we describe here provides a standard for characterizing infection and disease progression in this model.

## ACKNOWLEDGMENTS

We acknowledge Richard Herbert and all the veterinary staff at the NIH Animal Center. We thank Alicia Buckler-White, Ronald Plishka, Ranjini Iyengar, and all the staff of the NIAID LMM Core for assistance with viral loads and sequencing. We thank Vanessa Hirsch and Que Dang for providing SIVmac239 for inoculation in PTM. We thank the Cleveland Immunopathogenesis Consortium (BBC/CLIC) for advice and helpful discussions.

These studies were supported by the intramural program of the National Institute of Allergy and Infectious Diseases, U.S. National Institutes of Health, and in part by NIH grants R01-AI90797 to G. Silvestri and AI054292 to L. Picker as well as ONPRC Core grant RR00163.

The content of this publication does not necessarily reflect the views or policies of the Department of Health and Human Services, nor does mention of trade names, commercial products, or organizations imply endorsement by the U.S. Government.

## REFERENCES

1. **Agy MB, et al.** 1992. Infection of Macaca nemestrina by human immunodeficiency virus type-1. Science **257**:103–106.
2. **Alcantara S, et al.** 2009. Thrombocytopenia is strongly associated with simian AIDS in pigtail macaques. J. Acquir. Immune Defic. Syndr. **51**: 374–379.
3. **Batten CJ, et al.** 2006. Comparative evaluation of simian, simian-human, and human immunodeficiency virus infections in the pigtail macaque (Macaca nemestrina) model. AIDS Res. Hum. Retroviruses **22**:580–588.
4. **Beer BE, et al.** 2005. Immunodeficiency in the absence of high viral load in pig-tailed macaques infected with simian immunodeficiency virus SIVsun or SIVlhoest. J. Virol. **79**:14044–14056.
5. **Bontrop RE, Watkins DI.** 2005. MHC polymorphism: AIDS susceptibility in non-human primates. Trends Immunol. **26**:227–233.
6. **Bosch ML, et al.** 2000. Enhanced replication of HIV-1 in vivo in pigtailed macaques (Macaca nemestrina). J. Med. Primatol. **29**:107–113.
7. **Brenchley JM, et al.** 2004. T-cell subsets that harbor human immunodeficiency virus (HIV) in vivo: implications for HIV pathogenesis. J. Virol. **78**:1160–1168.
8. **Clark DR, de Boer RJ, Wolthers KC, Miedema F.** 1999. T cell dynamics in HIV-1 infection. Adv. Immunol. **73**:301–327.
9. **Clerici M, et al.** 2000. Immune activation in Africa is environmentally-driven and is associated with upregulation of CCR5. Italian-Ugandan AIDS Project. AIDS **14**:2083–2092.
10. **Desrosiers RC.** 1990. The simian immunodeficiency viruses. Annu. Rev. Immunol. **8**:557–578.
11. **Dietrich EA, et al.** 2011. Variable prevalence and functional diversity of the antiretroviral restriction factor TRIMCyp in Macaca fascicularis. J. Virol. **85**:9956–9963.
12. **Douek DC, et al.** 2002. HIV preferentially infects HIV-specific CD4+ T cells. Nature **417**:95–98.
13. **Douek DC, Picker LJ, Koup RA.** 2003. T cell dynamics in HIV-1 infection. Annu. Rev. Immunol. **21**:265–304.
14. **Edinger AL, et al.** 1997. Differential utilization of CCR5 by macrophage and T cell tropic simian immunodeficiency virus strains. Proc. Natl. Acad. Sci. U. S. A. **94**:4005–4010.
15. **Engram JC, et al.** 2009. Vaccine-induced, simian immunodeficiency virus-specific CD8+ T cells reduce virus replication but do not protect from simian immunodeficiency virus disease progression. J. Immunol. **183**:706–717.
16. **Favre D, et al.** 2009. Critical loss of the balance between Th17 and T regulatory cell populations in pathogenic SIV infection. PLoS Pathog. **5**:e1000295.
17. **Fernandez CS, et al.** 2011. Screening and confirmatory testing of MHC class I alleles in pig-tailed macaques. Immunogenetics **63**:511–521.
18. **Fernandez CS, et al.** 2005. Rapid viral escape at an immunodominant simian-human immunodeficiency virus cytotoxic T-lymphocyte epitope exacts a dramatic fitness cost. J. Virol. **79**:5721–5731.
19. **Giorgi JV, et al.** 1999. Shorter survival in advanced human immunodeficiency virus type 1 infection is more closely associated with T lymphocyte activation than with plasma virus burden or virus chemokine coreceptor usage. J. Infect. Dis. **179**:859–870.
20. **Goldstein S, et al.** 2005. Plateau levels of viremia correlate with the degree of CD4+-T-cell loss in simian immunodeficiency virus SIVagm-infected pigtailed macaques: variable pathogenicity of natural SIVagm isolates. J. Virol. **79**:5153–5162.
21. **Hatziioannou T, et al.** 2009. A macaque model of HIV-1 infection. Proc. Natl. Acad. Sci. U. S. A. **106**:4425–4429.
22. **Hunt PW, et al.** 2008. Relationship between T cell activation and CD4+ T cell count in HIV-seropositive individuals with undetectable plasma HIV RNA levels in the absence of therapy. J. Infect. Dis. **197**:126–133.
23. **Igarashi T, et al.** 2007. Human immunodeficiency virus type 1 derivative with 7% simian immunodeficiency virus genetic content is able to establish infections in pig-tailed macaques. J. Virol. **81**:11549–11552.
24. **Joag SV, et al.** 1997. Characterization of the pathogenic KU-SHIV model of acquired immunodeficiency syndrome in macaques. AIDS Res. Hum. Retroviruses **13**:635–645.
25. **Johnson PR, Goldstein S, London WT, Fomsgaard A, Hirsch VM.** 1990. Molecular clones of SIVsm and SIVagm: experimental infection of macaques and African green monkeys. J. Med. Primatol. **19**:279–286.
26. **Johnson PR, Hirsch VM.** 1991. Pathogenesis of AIDS: the non-human primate model. AIDS **5**(Suppl 2):S43–S48.
27. **Johnson PR, Hirsch VM.** 1992. SIV infection of macaques as a model for AIDS pathogenesis. Int. Rev. Immunol. **8**:55–63.
28. **Kemp K, Akanmori BD, Hviid L.** 2001. West African donors have high percentages of activated cytokine producing T cells that are prone to apoptosis. Clin. Exp. Immunol. **126**:69–75.
29. **Kent SJ, et al.** 1995. Cytotoxic and proliferative T cell responses in HIV-1-infected Macaca nemestrina. J. Clin. Invest. **95**:248–256.
30. **Klatt NR, et al.** 2010. Compromised gastrointestinal integrity in pigtail macaques is associated with increased microbial translocation, immune activation, and IL-17 production in the absence of SIV infection. Mucosal Immunol. **3**:387–398.
31. **Kubo M, et al.** 2009. Initiation of antiretroviral therapy 48 hours after infection with simian immunodeficiency virus potently suppresses acute-phase viremia and blocks the massive loss of memory CD4+ T cells but fails to prevent disease. J. Virol. **83**:7099–7108.
32. **Kuwata T, et al.** 2009. Association of progressive CD4(+) T cell decline in SIV infection with the induction of autoreactive antibodies. PLoS Pathog. **5**:e1000372.
33. **Lafont BA, Buckler-White A, Plishka R, Buckler C, Martin MA.** 2003. Characterization of pig-tailed macaque classical MHC class I genes: implications for MHC evolution and antigen presentation in macaques. J. Immunol. **171**:875–885.
34. **Lederer S, et al.** 2009. Transcriptional profiling in pathogenic and non-pathogenic SIV infections reveals significant distinctions in kinetics and tissue compartmentalization. PLoS Pathog. **5**:e1000296.
35. **Letvin NL.** 1990. Animal models for AIDS. Immunol. Today **11**:322–326.
36. **Loh L, Batten CJ, Petravic J, Davenport MP, Kent SJ.** 2007. In vivo fitness costs of different Gag CD8 T-cell escape mutant simian-human immunodeficiency viruses for macaques. J. Virol. **81**:5418–5422.
37. **Lukwiya M, et al.** 2001. Evaluation of immune activation in HIV-infected and uninfected African individuals by single-cell analysis of cytokine production. J. Acquir. Immune Defic. Syndr. **28**:429–436.
38. **Mandl JN, et al.** 2008. Divergent TLR7 and TLR9 signaling and type I interferon production distinguish pathogenic and nonpathogenic AIDS virus infections. Nat. Med. **14**:1077–1087.
39. **Mason RD, Rose RD, Seddiki N, Kelleher AD, Kent SJ.** 2008. Low pre-infection levels and loss of central memory CD4+ T cells may predict rapid progression in SIV-infected pigtail macaques. Virology **381**:11–15.
40. **Mattapallil JJ, et al.** 2005. Massive infection and loss of memory CD4+ T cells in multiple tissues during acute SIV infection. Nature **434**: 1093–1097.
41. **Mattapallil JJ, Letvin NL, Roederer M.** 2004. T-cell dynamics during acute SIV infection. AIDS **18**:13–23.
42. **McClure J, et al.** 2000. Derivation and characterization of a highly pathogenic isolate of human immunodeficiency virus type 2 that causes rapid CD4+ cell depletion in Macaca nemestrina. J. Med. Primatol. **29**: 114–126.
43. **Messele T, et al.** 1999. Reduced naive and increased activated CD4 and CD8 cells in healthy adult Ethiopians compared with their Dutch counterparts. Clin. Exp. Immunol. **115**:443–450.
44. **Miguez-Burbano MJ, Jackson J, Jr, Hadrigan S.** 2005. Thrombocytopenia in HIV disease: clinical relevance, physiopathology and management. Curr. Med. Chem. Cardiovasc. Hematol. Agents **3**:365–376.
45. **Naidu YM, et al.** 1988. Characterization of infectious molecular clones of simian immunodeficiency virus (SIVmac) and human immunodeficiency virus type 2: persistent infection of rhesus monkeys with molecularly cloned SIVmac. J. Virol. **62**:4691–4696.
46. **Newman RM, et al.** 2008. Evolution of a TRIM5-CypA splice isoform in old world monkeys. PLoS Pathog. **4**:e1000003.
47. **Okoye A, et al.** 2007. Progressive CD4+ central memory T cell decline results in CD4+ effector memory insufficiency and overt disease in chronic SIV infection. J. Exp. Med. **204**:2171–2185.

48. **O'Leary CE, et al.** 2009. Identification of novel MHC class I sequences in pig-tailed macaques by amplicon pyrosequencing and full-length cDNA cloning and sequencing. Immunogenetics **61**:689–701.
49. **Otten RA, et al.** 1994. Differential replication and pathogenic effects of HIV-1 and HIV-2 in Macaca nemestrina. AIDS **8**:297–306.
50. **Picker LJ, et al.** 2004. Insufficient production and tissue delivery of CD4+ memory T cells in rapidly progressive simian immunodeficiency virus infection. J. Exp. Med. **200**:1299–1314.
51. **Pitcher CJ, et al.** 1999. HIV-1-specific CD4+ T cells are detectable in most individuals with active HIV-1 infection, but decline with prolonged viral suppression. Nat. Med. **5**:518–525.
52. **Pratt BF, et al.** 2006. MHC class I allele frequencies in pigtail macaques of diverse origin. Immunogenetics **58**:995–1001.
53. **Rizzardini G, et al.** 1998. Immune activation in HIV-infected African individuals. Italian-Ugandan AIDS cooperation program. AIDS **12**: 2387–2396.
54. **Schmitz JE, et al.** 2009. Inhibition of adaptive immune responses leads to a fatal clinical outcome in SIV-infected pigtailed macaques but not vervet African green monkeys. PLoS Pathog. **5**:e1000691.
55. **Shibata R, et al.** 1999. Neutralizing antibody directed against the HIV-1 envelope glycoprotein can completely block HIV-1/SIV chimeric virus infections of macaque monkeys. Nat. Med. **5**:204–210.
56. **Silvestri G.** 2008. AIDS pathogenesis: a tale of two monkeys. J. Med. Primatol. **37**(Suppl 2):6–12.
57. **Silvestri G, et al.** 2003. Nonpathogenic SIV infection of sooty mangabeys is characterized by limited bystander immunopathology despite chronic high-level viremia. Immunity **18**:441–452.
58. **Smith MZ, et al.** 2005. Analysis of pigtail macaque major histocompatibility complex class I molecules presenting immunodominant simian immunodeficiency virus epitopes. J. Virol. **79**:684–695.
59. **Smith MZ, et al.** 2005. The pigtail macaque MHC class I allele Mane-A*10 presents an immunodominant SIV Gag epitope: identification, tetramer development and implications of immune escape and reversion. J. Med. Primatol. **34**:282–293.
60. **Virgen CA, Kratovac Z, Bieniasz PD, Hatziioannou T.** 2008. Independent genesis of chimeric TRIM5-cyclophilin proteins in two primate species. Proc. Natl. Acad. Sci. U. S. A. **105**:3563–3568.
61. **Zaunders JJ, et al.** 2001. Increased turnover of CCR5+ and redistribution of CCR5- CD4 T lymphocytes during primary human immunodeficiency virus type 1 infection. J. Infect. Dis. **183**:736–743.